Microwave Review
December 2023, Vol. 29, No. 2, pp. 71-82
DOI: 10.18485/mtts_mr.2023.29.2.9

An X/Ku-Band Series Feed Center Fed Shared Aperture Array Antenna for AIR-Borne Synthetic Aperture Radar Applications

Praveena Kati, Venkata Kishore Kothapudi

Astract – **A 5-element Shared Aperture Antenna Array for X/Ku-band Airborne synthetic aperture radar (AIR-SAR) applications is presented in this research work. As far as the authors are aware, few shared aperture antennas (SAA) exist that cover both X/Ku-band frequencies. The presented research is focused on designing a dual-band single linear-polarized (DBSP) series-fed center-fed (SFCF) X/Ku-band. The implementation of SAA is with the perception of an SFCF 5-element group as one group with three patches that are arranged orthogonal to each other to form two sets (3-patches) to realize a series fed array with coaxial probe feeding method in X/Ku-bands. The X-band (9.3 GHz) is best suited for soil moisture estimation in agricultural areas; the Ku-band (13.265 GHz): is mainly for snow and cold regions and disaster monitoring. The SAA prototype is fabricated and measured with S-parameters and radiation pattern characteristics to verify the antenna design concept, including gain measurements. The antenna exhibits -10 dB impedance bandwidth (BW) (9.1919-9.4674 GHz) (276 MHz with 2.96% BW) in X-band and (13.054-13.513 GHz) (459 MHz with 3.46% BW) in Ku-band. More than 25 dB of isolation has been measured between the ports and two separate bands in the same polarization. The antenna's X-band gain is 12 dBi at port-1 and its Ku-band gain is 11.3 dBi at port-2, according to the measurements. X-band side-lobe level (SLL) is better than -16.2 dB at port-1 and Ku-band SLL is better than -14.1 dB at port-2, as measured by SLL. The X/Ku-DBSP SAA has total dimensions of 120 × 60 × 1.6 mm^3 and for the presented design, measured and simulated results are in good agreement.**

Keywords – **Antenna; Shared Aperture; Array; Airborne Synthetic Aperture Radar; AIR-SAR**

I. INTRODUCTION

SAR technology by (Carl A. Wiley, 1954) observed airborne and spaceborne platforms, applying appropriate algorithms, SAR can provide a measure of earth's surface features and delineate subsurface level geophysical parameters. SAR emerged as a powerful operational research tool after the launch of Sea Sat SAR in 1978 (Holtet et al., 1992; Katsaros and Brown, 1991) spacecraft placed in a polar sun-synchronous orbit. Focus on the research area enables greater details with moderate resolution and more accuracy.

Article history: Received August 07, 2023; Accepted November 06, 2023

Praveena Kati and Venkata Kishore Kothapudi are with the Center of Excellence Advanced RF Microwave & Wireless Communications, Department of ECE, School of Electrical, Electronics, the Vignan's Foundation for Science, Technology, and Research, Guntur, India, -522213. E-mail: katipraveena@ieee.org

The single, double, and quad polarizations are required to be used for geophysical parameters using SAR [1]. The SAR is an antenna system that uses the Doppler Effect effectively. Many efforts have been made to increase and reduce the speckle noise by using spatial resolution SAR, which is an inherent part of SAR imaging, which collects information about a large range of objects by transmitting and receiving signals through the antenna arrays in the electromagnetic spectrum[2]. SAR systems provide geologist and terrain structural information for mineral discovery, The target's angular motion concerning the radar antenna is also used to create an image of the target [3]. Multiple feeding systems for shared-aperture antennae, such as parallel feed and series feed systems, provide adequate isolation between the three operation bands. The impedance bandwidths are 21 %, 11 %, and 18 % in the L, S, and X bands. The observed isolation in the three different bands is greater than 25 to 30 dB [4]. S-band and X-band dual band dual polarization (DBDP) microstrip antenna array frequencies 3.3 and 9 to 11 GHz, S-band uses probe feed patch and X-band patches are placed on top with the impedance matching bandwidth VSWR>2 and the bandwidth of S/X-band reaches 9.5% and 25%, isolation between two bands 15dB. Cross polarization of S-band ≤-21 dB and X-band ≤-20 dB [5]. A 2×3 array antenna has a large frequency range (2GHz) and helps to improve isolation between the elements. An array antenna has a frequency band (18.62 % fractional bandwidth) in the X/Ku bands [6]. Hybrid-fed shared aperture antenna with linear/circular polarization of X-band and linear polarization of K-band with 36 elements array and 10 element array, to reduce the SLL using series feed and coaxial fed in Chebyshev amplitude distribution to improve the side lobe levels of -25dB at K-band with scan angle 250, the bandwidth of 10.36/1.45% X/K-bands high efficiency 85% and gain of X/K-band 24.2/17.4 dBi [7]. S/X multilayer SAA, S-band antenna designed with cross-shaped proximity coupled square patch 4×4 planar array at S-band frequency of 2.7 GHz and X-band frequency of 9.7 GHz. S/X DBDP bandwidth 7.7/4.8%, isolation between two bands 25dB, Sidelobe levels of S-band and X-band -13/-15 dB, a gain of these bands are 8.48/21.8 dBi overall size of SAA 125×125×0.8 mm3[8].

Another article was designed with good isolation between bands and polarization and is best suited for the synthetic aperture antenna array. Construction size 100×100×1.6 mm^3 of antenna dual-band dual-polarized S/X single layer, X-band 2×2 subarray which makes 1×2 linear array at S-band antenna. Sidelobe levels are better than 17 dB, narrow bandwidth of the X-band of 9.3%, and an S-band bandwidth of 1.72% [9] [27]. A DBDP X-band linear and S-band circular polarization antenna. The X-band antenna is designed with stacked patches

to enhance gain and bandwidth. The bandwidth of 19.3/22 %, a gain of 10.8 dBi/5 dBi for S/X-bands, and isolation between two bands is 32 dB [10]. Circular polarization antenna array implemented C/X band, 2×2 arrays for C-band and 4×4 array for X-band same aperture for C-band circular patches itch at four corners and circular polarization. The result of antenna good isolation and low cross-polarization shows impedance bandwidth of 21% at the C-band 21.2 % at the X-band, Efficiency of 55%, low sidelobe levels of C-band, and X-band-12.5 and -15 dB, and gain for C-band 14.5 and X-band 17,5 dBi [11]. A tri-band dual-polarization (TBDP) L/S/X - bands measured results shows a good bandwidth of 13.4/ 14.8/16.8%, and array isolation/cross-polarization levels are better than 37 dB/-27 dB [12]. The antenna total height is about 80 mm at the lower frequency, cross polarization is better than 20dB in the P-band and 26 dB for Ku-band and measured gain better 8 dBi, aperture coupling patch of P-band and Ku band bandwidth 13% extending 330 to 420 MHz and sidelobe levels above -10 dB, design of antenna good for SAR applications, measured gain in the P-band ranged from 6.5 to 7.5 dBi. [13]. Another dual-polarized meta surface antenna made up of 4 patches, feed port efficiently exited one mode another mode cannot exit in patches are exited high isolation polarization levels, At the broadside, the enhanced cross-polarization levels are less than 40 dB. high impedance bandwidth of 36% and high isolation of <25 dB are both provided. [14].

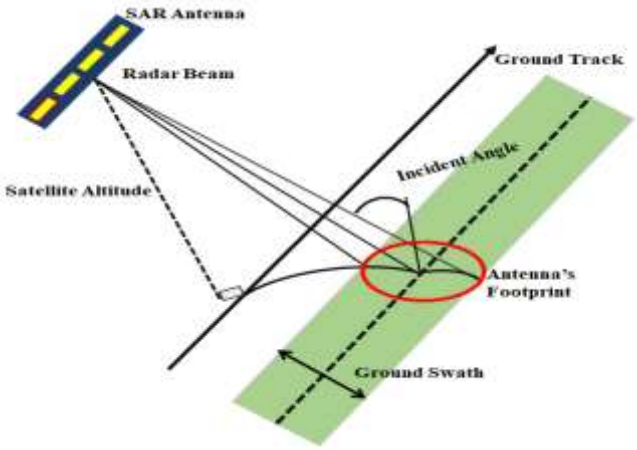

Fig. 1. Airborne synthetic apert radar geometry

Linear and circular polarization of S-band hybrid feed design 2×2, 3×3, and 6×6 arrays simulated and fabricated tested. The results of antenna Isolation are 45 and 43, cross-polarization levels are -36 dB, and a scan angle up to 45^0 is achieved these exited results depend on slot-coupled feed, respectively[15]. A three-layer SAA L/C-band is developed for SAR applications. The combination of patches and feed layers results in an exceedingly small antenna that is excellent for low-weight applications such as spaceborne SAR [16]. In [17], L and S bands, a dual-mode shared apert antenna consisting of two planer arrays of ring antennas is designed. The antennas are isolated and fed separately from one another. An L/C SAA is presented in [18], the sandwiched stacked patch is employed for the L-band element to increase bandwidth for a given element thickness. SAA with S and X Bands with Linear Polarization using a frequency ratio of 1:3.3 between the two bands saves space. The S-band antenna is the ground plane for a 2×2 X-band antenna array. The measured bandwidth (|S11|<-10 dB) in S-band is 13% and 6.2% in X-band due to patch electromagnetic coupling. It provides over 38 dB isolation throughout both frequency ranges. The S-band antenna gain is 7.5 dBi, while the X-band antenna gain is 10.5 dBi. The study recommends integrating the filter into the array's feed network for higher-order mode suppression. A microstrip filter is built into the antenna to reduce lower-order modes that interfere with higher-order modes used for SAA are in [19-22]. The proposed SAA has a frequency ratio of 1:1.8:4.5 for S/C/Ku triple-band (TB) dual-polarization (DP). The S-band array is built up of S-band-working shared items [23]. An integrated filtering duplex antenna was realized by attaching the duplexer to the dual-band patch through EM waves. [24]. In [31], the concept of a shared apert antenna was given as a basic understanding has been given.

TABLE 1
GENERAL SPECIFICATIONS SYNTHETIC APERT RADAR

Parameter	Value
Operating frequency	1-30 GHz (typical)
System bandwidth	100-200 MHz (typical)
Operating platform	Airborne
Platform altitude range	5-12.5 km/2-18 km (typical)
Modulations	Pulse, LFM, and pulse code
Mode of operation	Strip-mapping, squint, spotlight mode
Polarization	Linear/circular
Dynamic range and backscattering coefficient	20 to 40 dB (typical)
Spatial resolution	1-20 m (typical)
Swath width	5-60 km (typical)
Incidence angle	0^0 -80^0 (typical)
Pulse repetition frequency	4.2-5 kHz
Look angle	20^0 -35^0 (typical)
Receiver noise fig	3.5 dB (typical)
Platform speed	100 m/s

DBSP SAA is difficult on a single-layer PCB. It's redundant to have X and Ku band antennas. Antennas with shared apert are utilized. In the X and Ku bands, a single linear polarization with strong port isolation has been discussed extensively. The prototypes were tested in the lab. The proposed design could be employed in multi-frequency SAR systems. An X and Ku-band single-layer SAA with a single linear polarization is presented here. In practice, SAA was more vital in multifunctional radar systems. Prior research has focused on multi-layer architects with various frequency combinations. Several writers have reported the X/Ku-band SAA combination with various frequency ratios. An SAA with an FrequencyRatio of 1.426 requires only one layer of antennas. The present SAA architect has the following benefits: (1) X-band 5-element with series-feed Centre fed coaxial feed; (2) Efficient physical apert usage (3)

Coaxial probe feeding of 5-element planar arrays with series feeding (4) A 120×60×1.6 mm^3 apert (minimum) Fewer elements with appropriate gain and beam width, and a scanning capability of 25^0, enables for grating lobe free scanning. Due to its many feats, it is suited for the contemporary SAA design Table 1 summarizes the work's specs and design aims. X and Ku-band SAA antenna design prototype for SAR applications is provided in this study. The proposed antennas cover the 9.3/13.265 GHz X/Ku bands. The prototype is fabricated with a 1.6 mm substrate with 1-ounce copper makes them flexible. The prototypes are evaluated in an anechoic chamber and a VNA for S-parameter measurements. The calculations do not account for the effects of SMA connectors from microwave cables. We confirm an SAA design with reasonable performance. Section 2 describes SAR SAA geometry, while Section 3 describes X/Ku-band single-layer SAA geometry. Section 4 displays the antenna prototype and findings. Section 5 discusses potential improvement and scope. Section 6 concludes the research.

II. Shared Apert Antenna for Air-Sar

First-time sea-sat SAR provides synoptic image resolutions of the earth's surface, complex sensors, and major advanced technology for new dimensions observation monitor. Visible and infrared imagery later 1960 and 1970 passive sensors equal to angular resolution. Airborne and spaceborne active sensors are challenging areas of research. Scan, spotlight, strip map, and inverse SAR are four modes of SAR, the basic standard methods for obtaining images using interpolation and Fourier transform, one method is polar format algorithm spotlight mode collect histories another method tomographic. Developed airborne and spaceborne systems e.g., Tec SAR, in 1967-1988 RORSAR developed lupt1-5 used in military and civilian applications, Terra SAR-X and Tan DEM-X (X-band), SAR generates higher, day-and-night, climate change weather independent, environmental earth system monitoring, for various modes of mapping, and backscattering echoes are collected by the data, radar antenna transmission and reception time repeat for different positions. Envisat, notably the Radar sat Scans AR data, was introduced in 2003. The COSMO-Sky Med satellite constellation (X-band), ALMAZ-1, Radarsat-2 (C-band), Sea salt, and JERS-1, Terra SAR-X and Tan DEM-X (X-band), and Radarsat-2 (C-band), a new class of SAR satellites, began providing multi-mode SAR data in 2003. Terra SAR-X and Tan DEM-X (X-band), the COSMO-Sky Med satellite constellation (X-band), and Radarsat-2 are all examples of X-band radars (C-band). ERS-1 and -2 and Radarsat-1as well as Radarsat-1, have been operational and have provided significant volumes of SAR data [25,26]. AIR-SAR representation is shown in Fig 1 [1]-[9]. The General Specifications of SAR are shown in Table 1.

III. X/Ku-Band SAA Geometry and Configuration

The antenna material used in this study is RT/Duroid-5880 (Rogers) copper cladding substrate, 62 mils (1.574 mm) height, 1 ounce (0.035 mm) thick, with relative permittivity r = 2.2 and loss tangent tan = 0.0009 [29]. The overall size of the X/Ku-DBSP SAA is 120×60×1.6 mm^3 or (3.72×1.86×0.049) λ_0 (AIR as a medium) or (5.329×2.764×0.073) λ_g (substrate material as a medium), which corresponds to the X-band center frequency 9.3 GHz, (5.309×2.654×0.0707) λ_0 (AIR as a medium), (7.697×3.848×0.102) λ_g (substrate material as a medium), which corresponds to the Ku-band center frequency 13.265 GHz. All simulations are performed using the CST Microwave Studio student version [28].

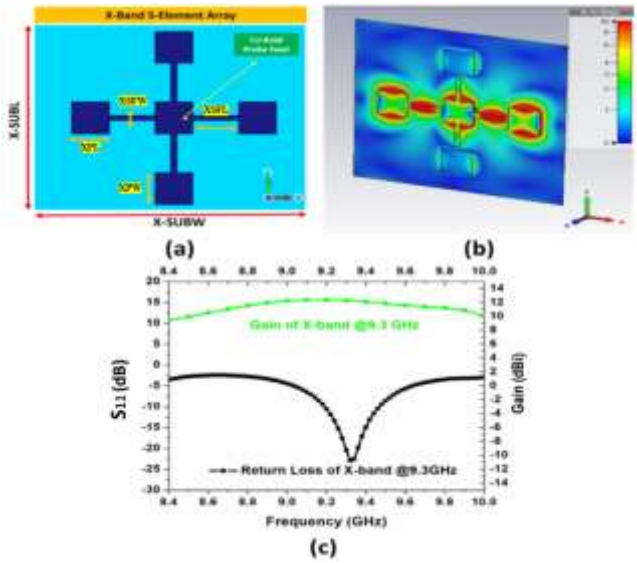

Fig. 2. (a) Geometry of X-Band, (b) Surface current distribution for X-band 5-element array design, (c) Simulated results of S_{11} and Gain versus frequency for X-Band 5-element array design.

TABLE 2
X/Ku-band SAA specifications

Parameters	X-Band	Ku-Band
Centre Frequency	9.3 GHz	13.265 GHz
Polarization	Linear	Linear
Impedance bandwidth	200 MHz	300 MHz
Antenna size	120×60×1.6 mm^3	
Radiation Efficiency	80 %	80 %
Gain	12 dBi	12 dBi
Isolation	>25 dB	>25 dB
Side-lobe level	-15 dB	-15 dB
Scan range	$+25^0$	$+25^0$
Cross-Polarization	>25 dB	>25 dB
Inter-element Spacing	0.7λ	0.7λ

Table-2 lists the linear polarized X/Ku-Band SAA specs. For X- and Ku-band, the resonance frequency is 9.3 and

13.265 GHz. Linear polarizations are expected in X-band (200 MHz) and Ku-band (300 MHz). Band isolation must be 25 dB. Specific AIR-SAR applications have led to the chosen frequency and beam pattern of the SAA for all activities.

A. X-Band 5-Element Design

The geometry of the 5-element X-band configuration is shown in Fig 2(a) with linear polarization including physical design parameters.

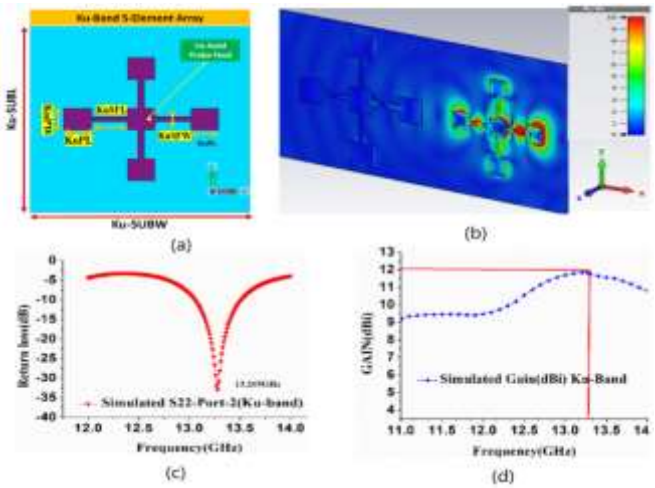

Fig. 3. (a) Geometry of Ku-Band, (b) Surface current distribution for Ku-band 5-element array design, (c) S_{22} and Gain versus frequency for Ku-Band 5-element array design

TABLE 3
OPTIMIZED PARAMETERS OF X/KU -SAA UNIT FOR X-BAND

Parameter	XPL	XPW	XSFL	XSFW
Value (mm)	10	10	12	1.6
Vale(λ_0)	0.31	0.31	0.372	0.049
Value(λg)	0.46	0.46	0.55	0.073
mm: millimeter				
λ_0: Free space wavelength λ_g: Guided wavelength				

The array is excited using a 50 Ω direct-coupled coaxial feeding at the middle patch for resonance with single linear polarization. The length and width of the series feed length is SFL=12 mm and SFW=1.2 mm to obtain the 50 Ω impedance matching and resonance at X-band, Table 3 shows optimized X/Ku-SAA values for X-Band. A coaxial feed is then employed to improve the desired antenna's impedance. The X-band SAA element distance can be calculated using Equations (1) respectively [7], [9].

$$d_x = \frac{\lambda x}{1+\sin\theta x} \quad (1)$$

The impedance bandwidth covers from 9.4674 – 9.1919 GHz (275.5 MHz) for $|S_{11}| < -10$ dB. Fig 2(c) shows the gain of the proposed 5-element X-band antenna array with a gain of 12 dBi. The polarization mechanism for S11-port is depicted in Fig 2(b) as surface current distribution (SCD). Fig 2(c) gives the S_{11} and gain performance of the X-band 5-element design. The $|S11| < -10$ dB plots show the best case with SFL =12 mm; guided wavelength (λ_g) = 21.7 mm at 9.3 GHz), and SFW is 0.2 mm (which is approximately 93.5 Ω). The frequency response of the S-parameter in the X-band element is shown in Fig 2(c), which indicates resonates at 9.3 GHz at single ports S11.

B. Ku-Band 5-Element Design

The configuration of the Ku-band 5-element antenna array is seen in Fig 3(a) with linear polarization including physical design parameters. The array is excited using a 50 Ω direct-coupled coaxial feeding at the middle patch for resonance with single linear polarization. The length and width of the series feed line are SFL=9 mm and SFW=1.2 mm to obtain the impedance of 50 Ω, Optimized Parameters of the X/Ku-SAA unit for Ku-Band are shown in Table 4. A coaxial feed is then employed to improve the desired antenna's impedance. The X-band SAA element distance can be calculated using Equations (2) respectively in [7][9].

$$d_{xKu} = \frac{\lambda xKu}{1+\sin\theta x} \quad (2)$$

The S_{22} and gain performance of Ku-band 5-element design. The $|S11| < -10$ dB plots show the best case with SFL =9 mm; guided wavelength (λ_g) = 15.59 mm at 13.265 GHz), and SFW is 0.2 mm (which is approximately 93.5 Ω). The polarization mechanism for S11-port is depicted in Fig 3(b) as Surface Current Distribution. The frequency response of the Ku-band 5-element is shown in Fig 3(c), which indicates that the antenna resonates at 13.265 GHz at a single port S22. The impedance bandwidth covers from 13.513 –13.054 GHz (459 MHz) for $|S22| <$ - 10 dB. Fig 3(c) shows the gain of the proposed 5-element Ku-band antenna array with a gain of 11.6 dBi.

TABLE 4
OPTIMIZED PARAMETERS OF X/KU -SAA UNIT FOR KU-BAND

Parameter	KuPL	KuPW	KuSFL	KuSFW
Value (mm)	7	7	9	1.2
Vale(λ_0)	0.309	0.309	0.398	0.053
Value(λg)	0.449	0.449	0.577	0.076
mm: millimeter λ_0: Free space wavelength concerning the velocity of propagation in air center frequency (3.2 GHz) (0.0226 meters) (22.6 millimeters) λ_g: Guided wavelength concerning the velocity of propagation in substrate material (RT-Duroid-5880) (0.01559 meters) (15.59 millimeters)				

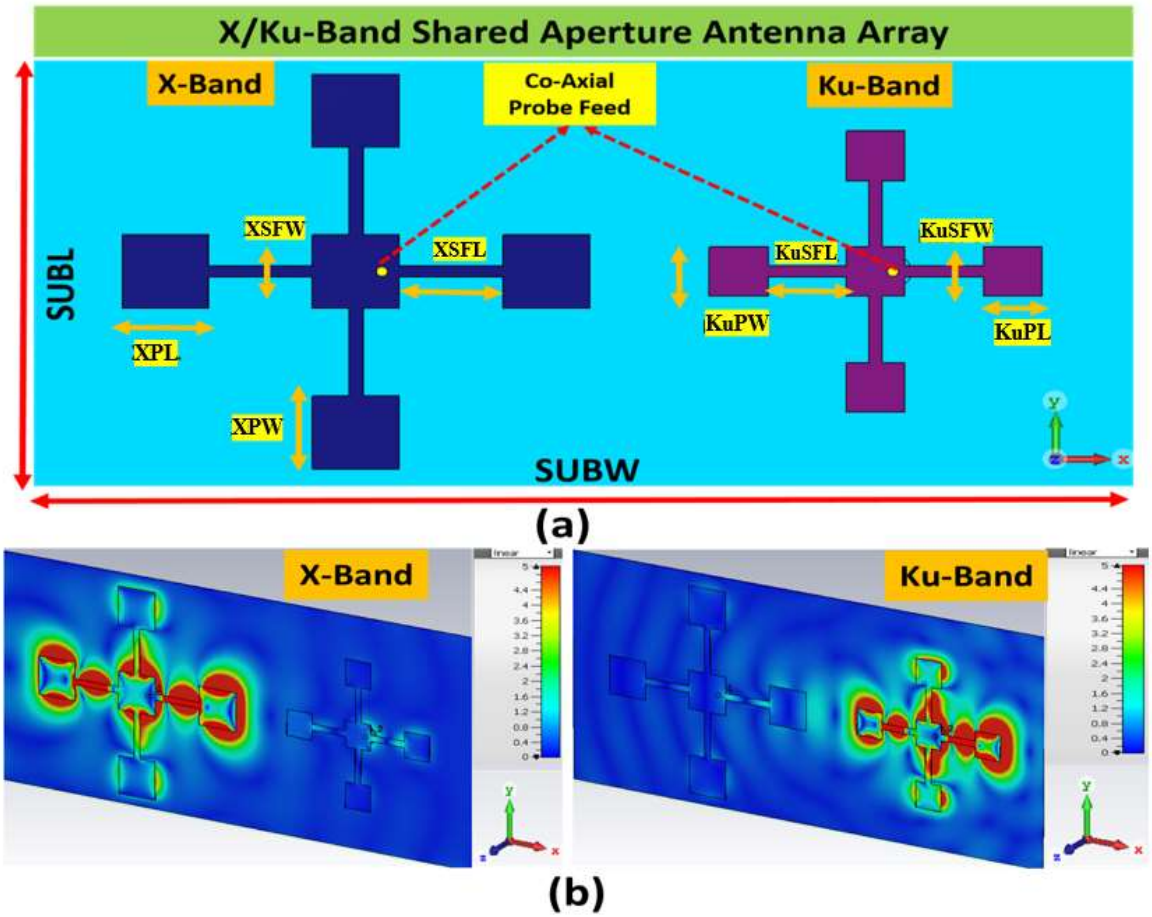

Fig. 4. (a) X/Ku-band shared apert antenna geometry, (b) Surface current distribution for X-band and Ku-band shared apert antenna array

C. Embedding X/Ku-Band DBSP-SAA

Fig 4 depicts the geometric arrangement of the proposed X/Ku-band SAA with a 5-element antenna array for each band in the proposed X/Ku-band SAA. An identical series-fed antenna array with a three-element group in both vertical and horizontal planes is used in the construction of the array, which has five group elements in total. The element group is implemented with linear polarisation. The feed width (SFW) of the series-fed X-band array has been optimized to 1.6 mm for maximum performance. An example of typical inter-element spacing 0.7λ used in an X-band array may be found in this SAA X-band antenna, which corresponds to a center frequency of 9.3 GHz (roughly one-guided wavelength), which is SFL = 12 mm in this SAA X-band antenna. When a narrow beam width and directivity are required, optimal spacing is used to reduce the number of antenna elements required. It consists of a 5-element group with an antenna that is fed by identical series-fed elements in each element. The different Parameters of the proposed substrate material are shown in Table-5. The element spacing of this SAA Ku-band linear array is 0.7λ, which translates to a resonance frequency of 13.265 GHz (roughly one guided wavelength). For a narrow beam and high directivity, the antenna components have been arranged at the optimal distance from one another. The CST software, which is a full-wave electromagnetic solution, is used throughout the entire design. Fig 4(a) and Fig 4(b) shows the design parameters geometry view of the X-band and Ku-band and surface current distribution respectively. Concerning propagation velocity, the overall size of the X/Ku-DBSP SAA is 120×60×1.6 mm^3. Because of the requirement for beam scanning, the distance between the elements is limited. The element distance for square distribution in X/Ku-band SAA on the X and Y axes can be calculated using the equations (3) respectively in [7][9].

$$d_x = \frac{\lambda x}{1+\sin\theta x} \quad \text{-----} \quad \text{-- (3)}$$

where λ_V and λ_H are the Vertical and Horizontal free-space wavelengths of 9.3 and 13.265 GHz. d_x and d_y are the distance between the elements in X-direction and Y-direction, Θ is the maximum scan angle of 250. The proposed SAA mutual coupling effect on both transmitting and receiving modes, antenna elements must be calculated to detect estimations mations of arrival, accuracy, and resolution. The isolation of the antenna depends on the correct calculation of current distribution on the complete body of the SAA, computing the SCD shown in Fig 4(b) takes the mutual coupling effect into account. Boundary conditions are not needed to be specified to reduce complexity and processing time.

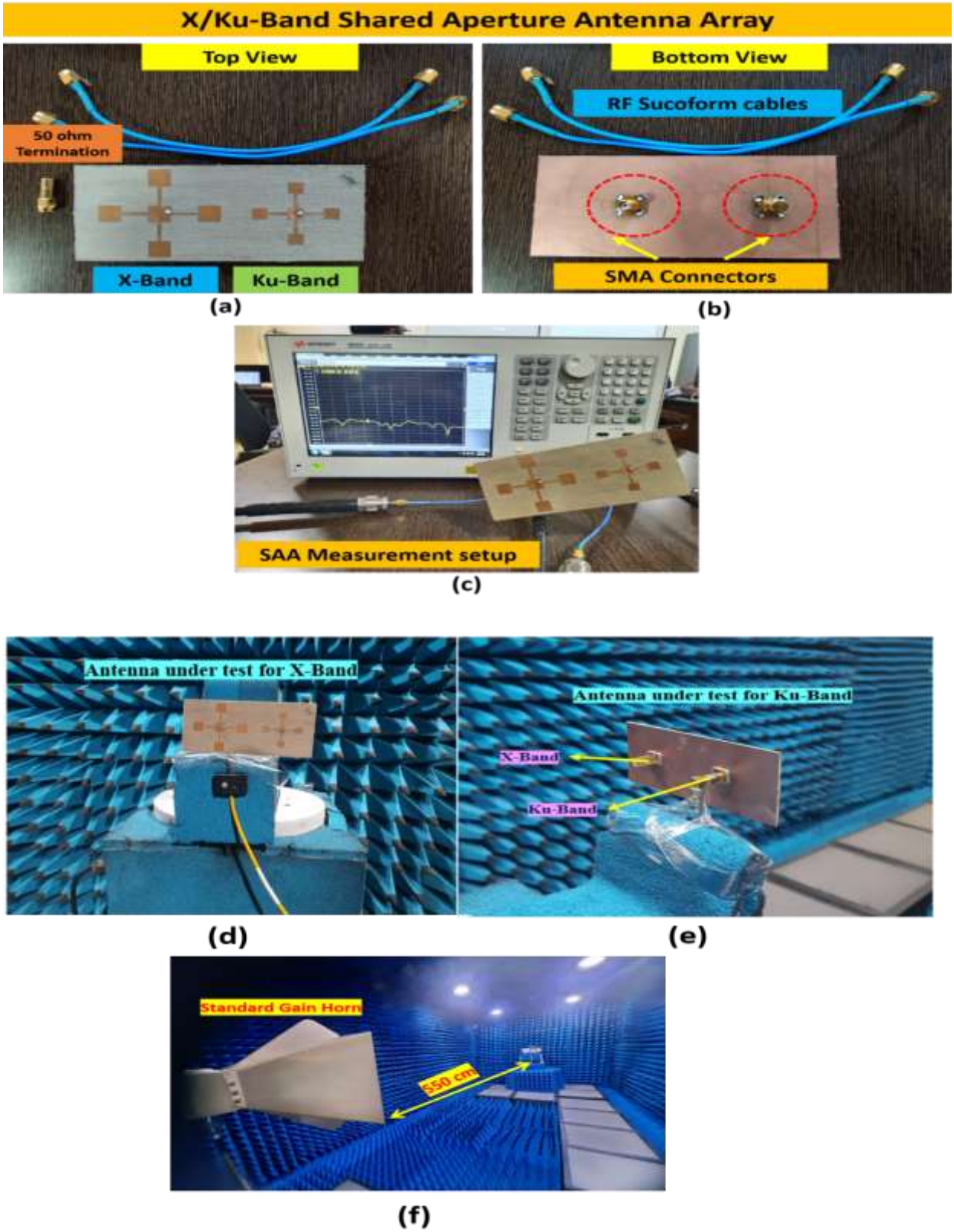

Fig. 5. Fabricated and measurement results phototype: (a) Top view of X/Ku-band SAA array, (b) Bottom view of X/Ku-band SAA, (c) Measurement setup with VNA, (d) Measurement setup in Anechoic chamber for X-band, (e) Measurement setup in Anechoic chamber for Ku-band, (f) Measurement setup using Standard horn Gain.

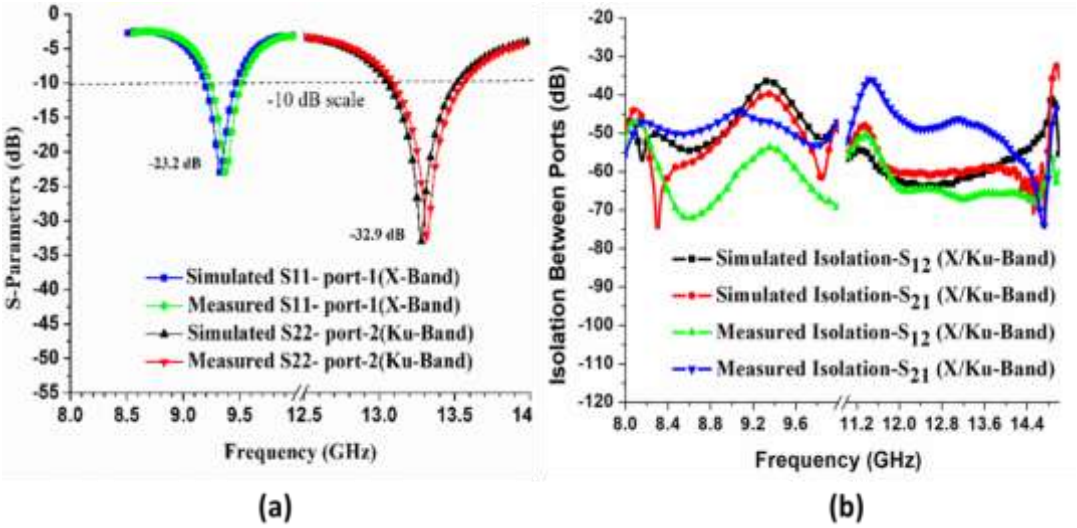

Fig. 6. (a) Simulated and measured S_{11} & S_{22} of X/Ku-band SAA, (b) Simulated and measured Isolation of X/Ku-band SAA

IV. Results and Analysis

X/Ku-DBSP single-layer SAA is constructed and experimentally validated in this work. Fig 5 (a-f) depicts the SAA prototype measuring setup, as well as top and bottom views of the apparatus and measurement setup for radiation patterns in an anechoic chamber X/Ku band and gain measurement setup. The scattering characteristics were measured using a network analyzer from the E5063A series of instruments. Figs 6 show the comparison of simulated and measured S-parameters i.e., $S_{11,}$ and isolation between bands at X/Ku-DBSP. The measured results match the models well. The notations of λx and λy denote the wavelength of the XZ-plane and YZ-plane for X/Ku-band SAA. Simulated and measured experimental S-parameters (S_{11}) of X/Ku-band shown in Fig-6(a), Simulated and measured Isolation between bands that port-1 (P1) and port-2 (P2) ($|S_{12}|=|S_{21}|$) shown in Fig-6(b), the return loss results show a -10dB bandwidth at port-1 S_{11} and port-2 S_{22}, X-band ranging from 9.1919-9.4674 GHz and the bandwidth of Ku-band ranging from 13.054-13.513 GHz. Isolation results between X/Ku-band over 48 dB. The distance between the transmitting antenna and receiving antennas is in the far-field region as shown in equation 4 in [30]. The radiation pattern is measd in an anechoic chamber using a standard gain horn antenna as the reference antenna having a gain (*Gr*) of 10 dBi at X/Ku-band. The reference antenna and proposed antenna are kept at a distance (*R*) of 550 cm. The power received by the horn antenna was -30 dBm for both cases, and the power received by the antenna under test (AUT) was around -28 dBm for X-band and -18.7 dBm for Ku-band. The transmitted power (*Pt*) is 0 dBm. The received power (*Pr*) is -30 dBm at X-band/Ku-band. The gain of the antenna under test (*Gt*) is calculated using the Friis transmission equation as follows in equation 5 in [30].

TABLE 5
Different Parameters of the Proposed Substrate Material

Substrate Material (RT/Duroid-5880) (L × W × H)					
Parameter	Value (mm)	Value (λ_0) @9.3 GHz	Value (λg) @9.3 GHz	Value (λ_0) @13.265 GHz	Value (λ_g) @13.265 GHz
L	120	3.72	5.529	5.309	7.697
W	60	1.863	2.764	2.654	3.848
H	1.6	0.049	0.073	0.0707	0.102
mm: millimeter; L: Length; W: Width; H: Height.					

$$r > 2D^2/\lambda \text{------} \quad \text{---------- (4)}$$

$$P_r = P_t G_t G_r \frac{\lambda^2}{4\pi R} \text{--------} \quad \text{-------- (5)}$$

Fig 7 (a-b) shows the simulated and measured X-band radiation pattern at 9.3 GHz. The antenna radiates well on the broadside. A 50 load on port 1 (X-band linear polarization) gives P1 a half-power beam width of 78.5^0 and a 12.3 dBi gain. A half-power beam width of 23.4^0 and a gain of 12 dBi are observed in the E-plane. In the H-planes, the observed SLL are under -16.2 dB and cross-pol levels are -30 dB (E-Plane), -21.7 dB (H-Plane). Both planes have an FTBR of 18 dB or higher. Fig 8 (a-b) shows the simulated and measured

TABLE 6
SUMMARY OF SIMULATION AND MEASURED RESULTS FOR X/KU-BAND SAA

Parameters		X-BAND		KU-BAND	
		Simulated	**Measd**	**Simulated**	**Measd**
Centre Frequency		9.3 GHz	9.3 GHz	13.265 GHz	13.265 GHz
Polarization		Linear	Linear	Linear	Linear
Impedance bandwidth		275 MHz	275 MHz	459 MHz	459 MHz
Isolation		50 dB	48 dB	50 dB	43 dB
Radiation Efficiency		93 %	92 %	94 %	92%
Gain		12.3 dBi	12 dBi	11.6dBi	11.3 dBi
E-Plane	Cross-Polarization	-35 dB	-26 dB	-35 dB	-29 dB
	HPBW	80.5^{o}	78.5^{o}	21.6^{o}	20.1^{o}
	Side Lobe Level	-16dB	-16.2dB	-16.8dB	-16.5dB
H-Plane	Cross-Polarization	-21.7 dB	-11.7 dB	-12 dB	-12 dB
	HPBW	22.2^{o}	23.4^{o}	78.9^{o}	76.6^{o}
	Side Lobe Level	-14 dB	-14.8 dB	-13.9 dB	-14.1 dB
Apert Area (AP)		$120\times60\times1.6mm^3$			

experimental Ku-band antenna radiation pattern at 13.265 GHz. The antenna has good HPBW and gains due to the increase in electrical size at high-band. The P1 is terminated with a 50 load for Ku-band linear polarization (P2). The antenna's HPBW is 20.1^0 and its gain is 11.3 dBi. The HPBW is 76.6^0 and the gain is 11.3 dBi. In the H-planes, SLL is -14.1 dB. The cross-pol is below -29 dB in the E and H planes at 13.265 GHz. FTBR > 18 dB in both planes. A standard gain is utilized as a reference antenna during the measurement of the gains. Fig 9 shows the simulated realized gains of this antenna. Peak gain is 12.3 dBi at 9.3 GHz, equivalent to efficiencies of 93/92 %. In the Ku-band, maximal linear polarization gains are around 11.6 dBi at % and 92%. Fig 10 depicts 3D radiation patterns. The X/Ku-band SAA S-parameters and radiation properties such as bandwidth, gain radiation efficiency, SLL, HPBW, and cross-pol, are determined and summarized in Table 6. GHz, equivalent to efficiencies of 94 % and 92%. Fig 10 depicts 3D radiation patterns. The X/Ku-band SAA S-parameters and radiation properties such as bandwidth, gain radiation efficiency, SLL, HPBW, and cross-pol, are determined and summarized in Table 6.

A single-layer antenna array is an element array in X and Ku bands. Compared to the SAAs in [5–11], [13], and [16–22], the suggested SAA has an FR of 1.426, better gains, and better band isolation. The dual-band prototype has a compact, multi-layer, planar SAA architect. Table 7 compares the SAA design to different SAA designs. We confirm an SAA design with reasonable performance. This design can be used to determine the best literary work.

V. DIRECTIONS OF IMPROVEMENT AND FUT SCOPE

AIR-SARs can employ SAA design principles here. They employ them differently depending on the criteria. The proposed design can also be modified by adding active and passive components. To merge the capabilities of several antennas into one apert, SAAs use wideband multiple-beam technology. Shared apert antennas decrease the number of related antenna systems by integrating many systems' functionalities into one.

- The proposed design can be implemented with 4 groups each with 5 elements to make a planar array and include the Ku-band 5-element array in the middle of the substrate using the coaxial feeding technique.
- Incorporated feeding network SAA design option Using SAA technology's integrated feeding network for loss and complexity reduction.
- Active modules, such as digital attenuators, are used to create multiple beams in Broadside and End-fire directions.
- Pair-wise anti-phase feeding method and differential feeding network for isolation and low cross-polarization improvement.
-
- Researching novel approaches to minimize SAA size and increase bandwidth.
- SAA was printed on RT-duroid in this work. In the fut, graphene nanofabrication can be designed. It is suitable for mm-wave SAR and automobile radar.

Today's airborne sensors can give high-quality SAR data with decimeters resolution, allowing for revolutionary SAR data processing and information extraction techniques and methodologies. High spatial resolution and innovative imaging techniques have made this possible.

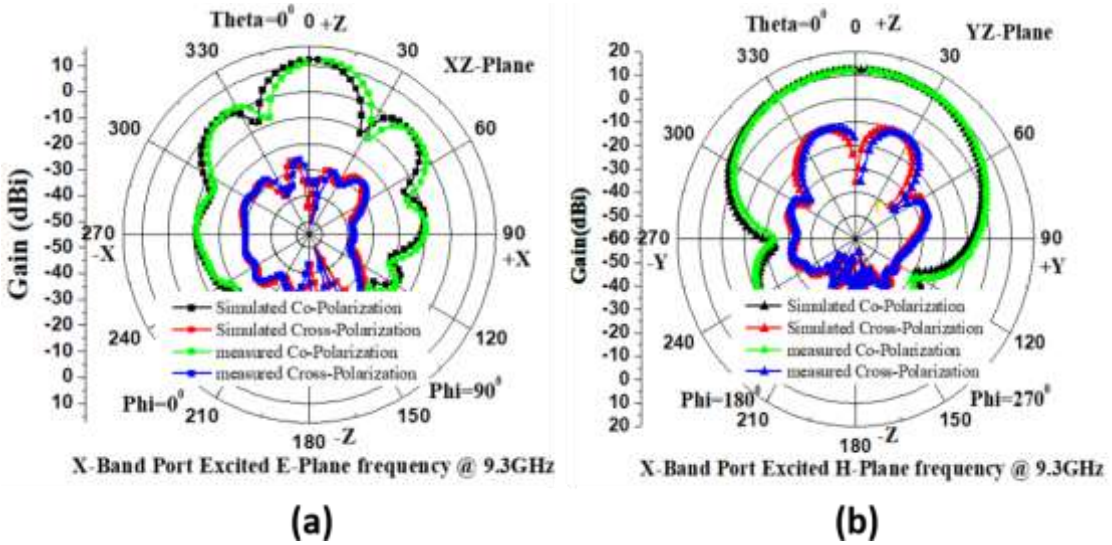

Fig. 7. Simulated & measured far-field Radiation Characteristics of X-Band 5-element array@ 9.3 GHz: (a) XZ-Plane (E-Plane), (b) YZ-Plane (H-Plane)

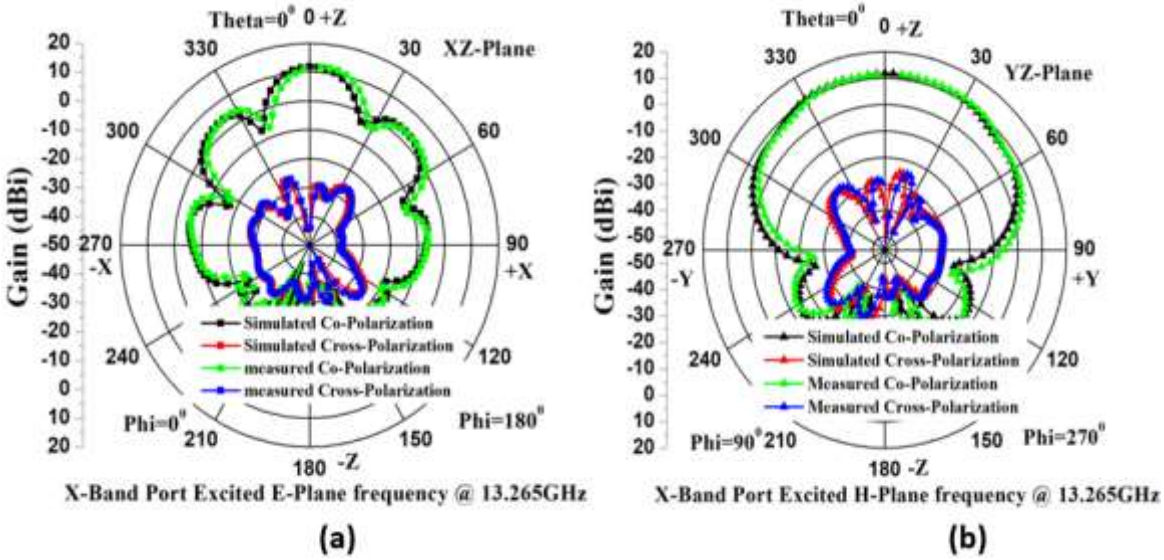

Fig. 8. Simulated & measured far-field Radiation Characteristics of Ku-Band 5-element array@ 13.265 GHz: (a) XZ-Plane (E-Plane), (b) YZ-Plane (H-Plane)

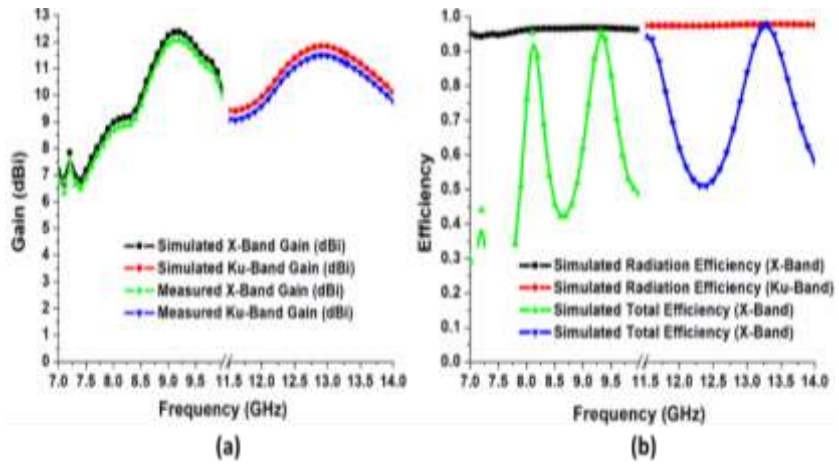

Fig. 9. (a) Simulated and Measured gain, (b) Simulated radiation efficiency of X/Ku-band SAA

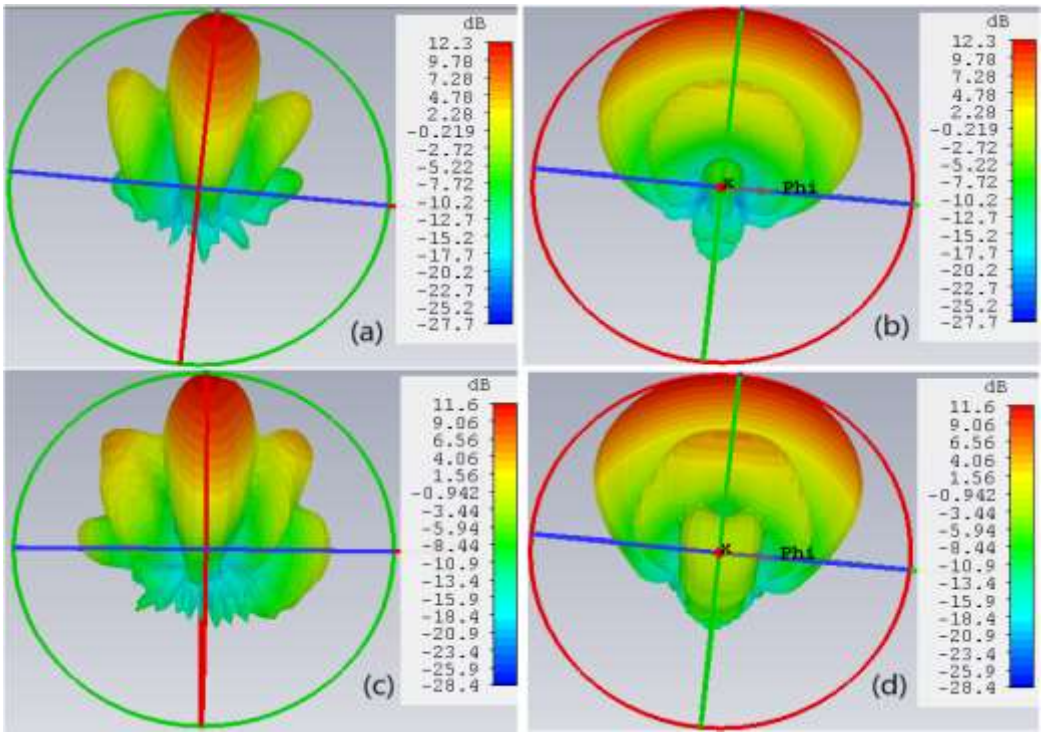

Fig. 10. 3D radiation patterns of Single-layer SAA design configuration at X/Ku-Band: (a) X-band- E-Plane, (b) X-Band-H-Plane, (c) Ku-Band-E-Plane and (d) Ku-Band-H-Plane.

TABLE 7
COMPARISON WITH OTHER SAA

Ref.	**Resonance Freq. (GHz)**	**Frequency Ratio**	**Dualband**	**Bandwidth (%)**	**Gain (dBi)**	**Isolation (dB)**	**Cross-pol (dB)**	**SLL (dB)**	**Size (λ)**
[5]	3-3.3/9-11	3.125	S/X	9.5/2	20.3	NA	21/20	-20/-10	1.11×1.92×0.018 λ^3
[7]	9.65/21	1:2.17	X/K	10.36/1.45	24.2/17.4	< 25	22/25	-18.9/-25	4.82×4.82×0.051 λ^3
[8]	2.7/9.7	1:3.59	S/X	7.7/4.8	8.48/21.8	< 25	-24/-20	-13/15	1.12×1.12×0.072 λ^3
[11]	5.3/8.2	1:1.54	C/X	21/21.2	14.5/17.5	<25	20	-12.5/-15	1.94×1.94×0.08 λ^3
[13]	450-730 MHz 34-36 GHz	NA	P/Ka	2.87-3.28 GHz	4.49-4./ 10.8-15.3	23.44	20/26	NA	NA
[18]	1.25/5.5	4.4	L/C	12.7/16.8	12.9/26.8	NA	-28/25 -28/28	NA	NA
[20]	2.5/8	3.2	S/X	7/10.5	8/11.5	30	NA	NA	1.166×1.166×0.53 λ^3
[21]	2.6-2.8/7.7-8.5	3	S/X	8.9/12.5	12.5/16.3	18/28	-18/-22	NA	1.23×1.23×0.007 λ^3
[22]	2.3-2.6/7.8-8.3	1:3.3	S/X	12.2/6.2	7.4/10	28/32	-17	NA	NA
This work	**9.3/13.265**	**1:1.4263**	**X/Ku**	**275/459 MHz**	**12.3/11.6**	**50**	**-11.7/12**	**-16.2 /14.1**	**3.72×1.86×0.04 λ^3**

VI. CONCLUSION

This article presents an SAA with X/Ku-band single linear polarized design with a single layer. For X/Ku bands, the square patches form a 5-element series-fed array activated by a coaxial probe. The X/Ku band feeding systems are etched on the same layer to maintain adequate band separation. The existing X/Ku SAA is modeled, built, and tested, with matching bandwidths of 2.96% and 3.46% at X/Ku-bands. In X/Ku bands, P1 and P2 are Isolation between Ports 50 dB apart. In addition to SLL, gain, efficiency, and cross-pol radiation performance are excellent. The X/Ku-band SAA is tiny, measuring 120x60x1.6 mm^3. The SAA prototype design was compact, easy to model, and single layer, making it suitable for big SAA for ASAR systems. Due to cost and facility constraints, the authors built the proof-of-concept prototype with minimal elements and achieved appropriate electrical (S-parameters) and radiation characteristics when compared to simulated and measured findings. This SAA can be extended to large arrays in the fit for AIR-SAR.

REFERENCES

[1] V. K. Kothapudi, V. Kumar, "Shared Aperture Antenna Technology for SAR: A Review of the Theory and Applications", *Journal of Engineering Science and Technology Review*, vol. 10, pp. 41–54, 2017.

[2] A. Javali, J. Gupta, and A. Sahoo, "A Review on Synthetic Aperture Radar for Earth Remote Sensing: Challenges and Opportunities," *2021 Second International Conference on Electronics and Sustainable Communication Systems (ICESC)*, pp. 596–601, 2021.

[3] V. M. Patel, G. R. Easley, D. M. Healy, and R. Chellappa, "Compressed Synthetic Aperture Radar," *IEEE Journal of Selected Topics in Signal Processing*, vol. 4, no. 2, pp. 244–254, 2010.

[4] K. Li, T. Dong, and Z. Xia, "A Broadband Shared-Aperture L/S/X-Band Dual-Polarized Antenna for SAR Applications," *IEEE Access*, vol. 7, pp. 51417–51425, 2019.

[5] S.-H. Hsu, Y.-J. Ren, and K. Chang, "A Dual-Polarized Planar-Array Antenna for S-Band and X-Band Airborne Applications", *IEEE Antennas and Propagation Magazine*, vol. 51, no. 4, pp. 70–78, 2009.

[6] M. Alibakhshikenari, B. S. Virdee, C. H. See, R. A. Ab_Alhameed, F. Falcone, and E. Limiti, "Array Antenna for Synthetic Aperture Radar Operating in X and Ku-Bands: A Study to Enhance Isolation Between Radiation Elements", *12th European Conference on Synthetic Aperture Radar*, 2018.

[7] V. K. Kothapudi, V. Kumar, "Hybrid-Fed Shared Aperture Antenna Array for X/K-Band Airborne Synthetic Aperture Radar Applications," *IET Microwaves, Antennas & Propagation*, vol. 15, Dec. 2020.

[8] V. K. Kothapudi, P. Kati; B. A. Nunna, P. S. Mindala, A. Kayithi, S. R. Shivagari, H. V. P. R. Kandhi, B. Meesala, Y. R. Tiyyagura, S. R. Eduru, "An S/X-band Multi-layer Shared Aperture Antenna with Frequency Ratio of 2.9 for Airborne Synthetic Aperture Radar Applications," *2021 Photonics Electromagnetics Research Symposium (PIERS)*, pp. 1406–1411, 2021.

[9] V. K. Kothapudi, V. Kumar, "A Single Layer S/X-band Series-Fed Shared Aperture Antenna for SAR Applications," Progress In Electromagnetics Research C, vol. 76, pp. 207–219, Jan. 2017.

[10] K. Wang, X.-L. Liang, W. Zhu, J. Geng, L. Jianping, Z. Ding, R. Jin, "A Dual-Wideband Dual-Polarized Aperture-Shared Patch Antenna With High Isolation," *IEEE Antennas and Wireless Propagation Letters*, vol. 17, no. 5, pp. 735–738, 2018.

[11] C.-X. Mao, S. Gao, Y. Wang, Q.-X. Chu, and X.-X. Yang, "Dual-Band Circularly Polarized Shared-Aperture Array for C-/X-Band Satellite Communications," *IEEE Transactions on Antennas and Propagation*, vol. 65, no. 10, pp. 5171–5178, 2017.

[12] S.-S. Zhong, Z. Sun, L.-B. Kong, C. Gao, W. Wang, and M.-P. Jin, "Design of TBDP Shared-Aperture SAR Array," *Asia-Pacific Microwave Conference*, pp. 159–162, 2011.

[13] D. Park, J. Choi, "A Dual-Band Dual-Polarized Antenna with Improved Isolation Characteristics for Polarimetric SAR Applications," *Applied Sciences*, vol. 11, no. 21, 2021.

[14] S. Liu, D. Yang, Y. Chen, X. Zhang, and Y. Xiang, "High Isolation and Low Cross-Polarization of Low-Profile Dual-Polarized Antennas via Meta surface Mode Optimization", *IEEE Trans. Antennas Propagation*, vol. 69, no. 5, pp. 2999–3004, May 2021.

[15] H. Saeidi-Manesh, G. Zhang, "High-Isolation, Low Cross-Polarization, Dual- Polarization, Hybrid Feed Microstrip Patch Array Antenna for MPAR Application", *IEEE Trans. Antennas Propagation*, vol. 66, no. 5, pp. 2326–2332, May 2018.

[16] G. Vetharatnam, V. Koo, "Compact L- & C-band SAR Antenna," *Progress in Electromagnetics Research Letters*, vol. 8, pp. 105–114, Jan. 2009.

[17] J. Dhiman, A. Sharma, and S. Khah, "Shared Aperture Microstrip Patch Antenna Array for L And S-Bands," *Progress In Electromagnetics Research Letters*, vol. 86, pp. 91–95, Jan. 2019.

[18] Z. Sun, K. P. Esselle, S. Zhong, and Y. J. Guo, "Shared-Aperture Dual-Band Dual-Polarization Array Using Sandwiched Stacked Patch," *Progress in Electromagnetics Research C*, vol. 52, pp. 183–195, 2014.

[19] P. Mathur and G. Kumar, "Antenna at S-Band as Ground for Array at X-Band in Dual Frequency Antenna at S/X-Bands", *Progress In Electromagnetics Research Letters*, Vol. 71, pp. 15-22, 2017.

[20] P. Mathur, G. Kumar, "Dual-Frequency Microstrip Antenna at S And X Bands with Higher-Order Mode Suppression Technique," *IET Microwaves, Antennas & Propagation*, vol. 12, no. 4, pp. 583–587, 2017.

[21] P. Mathur, G. Kumar, "Dual-Frequency Dual-Polarised Shared-Aperture Microstrip Antenna Array with Suppressed Higher Order Modes," *IET Microwaves, Antennas & Propagation*, vol. 13, no. 9, pp. 1300–1305, 2019.

[22] P. Mathur, G. Kumar, "Dual-Band Dual-Polarized Microstrip Antenna at S- And X-Bands Using Feed Technique for Suppression of Interference Due To Higher Order Modes," *International Journal of RF and Microwave Computer-Aided Engineering*, vol. 31, no. 11, p. e22870, 2021.

[23] J. Xu, C.-Jiang Guo, and J. Ding, "Compact Tri-Band Dual-Polarized Shared Aperture Array", *Progress In Electromagnetics Research M*, vol. 104, pp. 101-110, 2021.

[24] M. G. Aly, C. Mao, S. Gao, and Y. Wang, "A Ku-Band Filtering Duplex Antenna for Satellite Communications", *Progress In Electromagnetics Research M*, vol. 85, pp.1-10, 2019.

[25] A. Moreira, P. Prats-Iraola, M. Younis, G. Krieger, I. Hajnsek, and K. Papathanassiou, "A Tutorial on Synthetic Aperture Radar," *IEEE Geoscience and Remote Sensing Magazine (GRSM)*, vol. 1, pp. 6–43, Mar. 2013.

[26] C. Zhou, F. Deng, L. Wan, Z. Wang, D. E, and Y. Zhou, "Application of Synthetic Aperture Radar Remote Sensing in Antarctica," *Remote Sensing of the Environment: 18th National*

Symposium on Remote Sensing of China, vol. 9158, pp. 123–130, 2014.
[27] V. K. Kothapudi, V. Kumar, "Compact 1 × 2 and 2 × 2 Dual Polarized Series-Fed Antenna Array for X-Band Airborne Synthetic Aperture Radar Applications," *Journal of Electromagnetic Engineering and Science*, vol. 18, pp. 117–128, Apr. 2018
[28] *Computer simulation technology version (2018)*, Wellesley Hill MA. Available At: www.cst.com
[29] *Rogers Corporation*, Available At: www.rogerscorp.com
[30] C. A. Balanis, *Antenna theory: Analysis and design. Antennas & Propagation. 4th edn*. Wiley, Hoboken (1997)
[31] C. I. Coman, I. E. Lager, and L. P. Ligthart, "The Design of Shared Aperture Antennas Consisting of Differently Sized Elements," *IEEE Transactions on Antennas and Propagation*, vol. 54, no. 2, pp. 376–383, Feb. 2006.